

# Biomimetic modification of poly-L-lysine and electrodeposition of nanocomposite coatings for orthopaedic applications

A. Clifford<sup>a</sup>, B.E.J. Lee<sup>b</sup>, K. Grandfield<sup>a,b</sup>, I. Zhitomirsky<sup>a,b,\*</sup>

<sup>a</sup> Department of Materials Science and Engineering, McMaster University, Hamilton, Ontario, L8S4L7, Canada

<sup>b</sup> School of Biomedical Engineering, McMaster University, Hamilton, Ontario, L8S4L7, Canada

---

## ARTICLE INFO

### Keywords:

Poly-L-lysine Catechol Hydroxyapatite Rutile

Electrophoretic deposition Film

## ABSTRACT

For the first time, a biomimetic method has been developed for the chemical modification of poly-L-lysine (PLL) with catechol in order to improve polymer adhesion to inorganic particles and surfaces. The method is based on the Schiff base reaction of amino groups of PLL monomers and aldehyde groups of 3,4-dihydroxybenzaldehyde (DHBA) molecules. It was found that adherent PLL-DHBA films can be prepared by cathodic electrophoretic deposition (EPD). Nanocomposite coating with dual micro-nano topography has been developed for orthopaedic and dental coating applications. The catechol groups of PLL-DHBA facilitated its adsorption on hydroxyapatite (HA) and rutile (TiO<sub>2</sub>) and allowed the fabrication of stable suspensions for EPD. PLL-DHBA was used as both a charging and film-forming agent for EPD of HA and TiO<sub>2</sub>. Moreover, the methods allowed co-deposition of HA and TiO<sub>2</sub> and fabrication of composite films, which allows the benefits of both bioceramics to be combined. In addition to having dual scale topography, the films exhibited both sub-micron surface roughness and hydrophilic behaviour, which both have been found to promote osteoblast adhesion and proliferation. *in vitro* studies revealed that the fabricated coatings showed increased cell metabolism and alkaline phosphatase activity over the period studied, with PLL-DHBA-TiO<sub>2</sub> showing the greatest increase. This work paves the way for both the development of the next generation of biomedical implant coatings, with improved osseointegration and lifespan, as well as one-step low-temperature processing.

## 1. Introduction

Poly-L-lysine (PLL) is a cationic biopolymer that is synthesized from L-lysine, a naturally occurring essential amino acid found in food sources with high protein content, such as meat and eggs [1]. It has also been found to have anti-microbial properties [2,3], which makes it well suited for biomedical applications. The amine group in PLL is protonated in biological conditions and has been found to promote cell proliferation and adhesion [4]. As a result, PLL is commonly used as a coating agent in tissue culture equipment [5]. PLL has been used for a variety of biomedical applications, such as tissue scaffolds [2,3], drug delivery [4], cell labeling [6] and gene delivery [7]. PLL is also being explored for bone scaffold and orthopaedic coating applications, as it is believed to promote proliferation and adhesion of osteoblasts due to its peptide structure [4].

Recent interest has been generated in the area of biopolymer modification with catechol (CAT), in order to improve polymer adhesion to inorganic particles and surfaces. This interest is inspired by nature; observing the ability of the mussel to cling to inorganic surfaces in aggressive marine environments. This ability has been attributed to the presence of L-3,4-dihydroxyphenylalanine (L-DOPA), an amino acid that is the primary constituent of the adhesion protein in the byssal plaque [8]. The naturally occurring biopolymer, chitosan (CHIT) has been modified previously with CAT using a variety of techniques for modification, including reductive amination or chemical, enzymatic, or electrochemical synthesis [9]. A two-step method for electrochemical synthesis has been described, which involves the cathodic electro-deposition of chitosan, followed by anodic deposition of catechol [10]. We have previously developed a new one-step technique for the modification of CHIT, utilizing the CAT containing organic compound 3,4-dihydroxybenzaldehyde (DHBA) [11]. In our technique, CHIT-DHBA was fabricated by attaching DHBA to CHIT monomer at the amine group, utilizing a Schiff base reaction. CHIT-DHBA films were then fabricated using cathodic electrophoretic deposition (EPD).

EPD is an attractive coating technique for orthopaedic and dental implants due to its ability to coat substrates with complex shapes and incorporate multiple components while being relatively cheap and facile [12]. PLL films have previously been fabricated using EPD [13]. In this technique, it was suggested that the amino group of PLL became protonated upon the dissolution of PLL-hydrobromide in water, forming PLL-H<sup>+</sup>. PLL-H<sup>+</sup> then migrated towards the cathode under the influence of an applied electric field. The application of the electric field results in local increase in pH at the cathode surface, governed by the following reaction



As PLL polyelectrolyte enters the locally alkaline region at the cathode surface, it becomes deprotonated



and coagulates on the cathode surface, forming an electrically neutral and water insoluble film. Using this method, PLL has been used for the fabrication of organic-inorganic composite films with hydroxyapatite (HA) [13], which is a synthetic bioceramic that has a chemical composition similar to the inorganic constituent in human bone [14]. There are no reports of the use of PLL for the electrodeposition or co-deposition of inorganic particles besides the aforementioned HA.

The goal of this investigation was to fabricate and characterize catechol-modified PLL composite films using a one-step electrodeposition technique and determine their feasibility for use as orthopaedic and dental implant coatings. In our work, we functionalized PLL with catechol and formed composite films with HA, and rutile (TiO<sub>2</sub>). We also achieved co-deposition of HA with TiO<sub>2</sub>, and fabricated coatings with dual nano- and micro-scale topography in one step, which was found to promote adhesion and proliferation of osteoblast-like Saos-2 cells. This work paves the way for the fabrication of a new generation of nano-composite coatings with superior adhesion and dual-scale topography for improved osseointegration and

increased lifespan of biomedical implant materials.

## 2. Experimental procedure

### 2.1. Chemicals

Poly-L-lysine hydrobromide (PLL-HBr), 3,4-dihydroxybenzylaldehyde (DHBA), TiO<sub>2</sub> (rutile, < 100 nm), Ca(NO<sub>3</sub>)<sub>2</sub>·4H<sub>2</sub>O, (NH<sub>4</sub>)<sub>2</sub>HPO<sub>4</sub>, NH<sub>4</sub>OH and titanium foil (0.127 mm) were purchased from Sigma-Aldrich Canada. HA nanorods were synthesised using wet chemical precipitation [15]. A solution consisting of 0.6 M (NH<sub>4</sub>)<sub>2</sub>HPO<sub>4</sub> was slowly added to 1.0 M Ca(NO<sub>3</sub>)<sub>2</sub> solution at 70 °C. The solution pH was adjusted to 11 using NH<sub>4</sub>OH and was stirred for 8 h at 70 °C, followed by stirring for 24 h at room temperature. The average length of the synthesized HA nanorods was approximately 169 ± 15 nm, and the average width was approximately of 31 ± 1.4 nm.

PLL-DHBA films were fabricated by first dissolving PLL-HBr and DHBA into deionized water, forming aqueous solutions of PLL and DHBA with final concentrations of 1 g L<sup>-1</sup> and 5 g L<sup>-1</sup> respectively. Upon the dissolution of PLL-HBr in DI water, the amine group became protonated, forming cationic PLL. PLL was modified in the liquid state utilizing a Schiff base reaction with DHBA solution, using a 2:1 mass ratio of PLL to DHBA. The resulting solution obtained a yellow hue and was diluted with anhydrous ethanol, with a final concentration of 70% ethanol-30% water, for the fabrication of PLL-DHBA films using cathodic EPD.

### 2.2. Electrochemical coating fabrication

Ti foil was used as both the film substrate and cathode in the electrochemical cell set-up. Pt counter electrodes were located 15 mm on either side of the Ti cathode. All coatings were deposited at 50 V, and pure PLL-DHBA films were fabricated. In addition to pure PLL-DHBA films, composite films containing hydroxyapatite (HA), rutile (TiO<sub>2</sub>) and a combination of both HA and TiO<sub>2</sub> were fabricated using cathodic EPD. The concentration of HA or TiO<sub>2</sub> nanoparticles dispersed in the PLL-DHBA solution was 1 g L<sup>-1</sup>.

### 2.3. Coating characterization

A JEOL 7000 F scanning electron microscope (SEM) was used to characterize the surface coating morphology. Atomic force microscopy (AFM) was used to determine the surface roughness, and all measurements were carried out using a Bruker Bioscope Catalyst atomic force microscope. The area probed on each surface was equal to 22.5 mm<sup>2</sup>, and the average roughness for each surface was calculated from this area. The sessile drop method was used to characterize the wettability of the PLL-DHBA coatings. An OCA 35 contact angle measuring device was used to conduct the experiment. To take a measurement, three microlitres of deionized water was dropped onto the sample surface and the contact angle on the left and right side of the drop was calculated immediately upon contact using the corresponding contact angle measurement software, SCA 20. Readings were taken from five different areas of the sample, and the average wetting angle was calculated from these measurements. Coating adhesion was measured according to the procedure outlined in ASTM standard D3359-09. An Aligent Carry 5000 spectrometer was used for ultraviolet-visible (UV-vis) spectroscopy measurements. PLL, DHBA, and PLL-DHBA dissolved in ethanol solution were analyzed in matching 10 mm quartz cuvettes, using dual beam mode. Fourier transform infrared spectroscopy measurements were obtained using a Bruker Vertex 70 Spectrometer. A powder diffractometer equipped with a Rigaku Cu K $\alpha$  rotating anode and a Bruker SMART6000 CCD were used for X-ray diffraction experiments.

### 2.4. Cell culturing

Saos-2 cells were grown in McCoy's 5 A modified media in 15% fetal bovine serum and 1% penicillin/streptomycin. Cells were obtained from ATCC<sup>®</sup> while other cell culture reagents were obtained from Life Technologies Inc. Cells were maintained at 37 °C with 5% CO<sub>2</sub> and media was exchanged every 4 days. Once a confluent cell monolayer was obtained, cells were detached with trypsin in 0.25% ethylenediaminetetraacetic acid (EDTA) EPD film samples (15 mm diameter) were placed in a 24 well plate and cells were plated at a density of 10,000 cells/cm<sup>2</sup>. All samples were sterilized under UV radiation for 15 min prior to cell seeding. Cells were counted using an Invitrogen Countess Automated Cell Counter. Cells grew on the surfaces of the films for 1 and 3 days. 5 samples were used for each film and time point combination. Methods were similar to those used in previous published work [16].

### 2.5. Cell metabolism

Cell metabolism was measured using an alamarBlue<sup>®</sup> dye obtained from Life Technologies Inc. alamarBlue<sup>®</sup>, or resazurin, is only converted to the fluorescent resorufin when it interacts with metabolizing cells which allows for it to be an indication of cellular activity. The pre-existing media was removed from each well and was subsequently replaced by 650  $\mu$ L of a 5% alamarBlue solution (in McCoy's 5 A media). The samples were incubated in the dark for 1 h at 37 °C with 5% CO<sub>2</sub>. Fluorescence values were determined using a Tecan Infinite<sup>®</sup> M1000 at 540–580 nm (excitation-emission). The blank reading was subtracted from each value to obtain the signal corresponding to the cells only. Following plate reading, the alamarBlue solution was removed and 300  $\mu$ L of 0.1% triton lysis solution (in PBS) was added to each well in preparation for additional assays.

### 2.6. Alkaline phosphatase activity

Alkaline phosphatase (ALP) activity was measured using the ALP assay from Abcam<sup>®</sup>. P-nitrophenol phosphate powder was dissolved in ALP assay buffer to prepare incubation solution. The phosphate group is cleaved off in the presence of alkaline phosphatase and the resulting p-nitrophenol emits light. 25  $\mu$ L of lysed cells in PBS was added to a 96 well plate, in triplicate, for each sample. Subsequently, 50  $\mu$ L of incubation solution was added to each well and the plate was incubated for 20 min in the dark at 37 °C with 5% CO<sub>2</sub>. Absorbance was read using a Tecan Infinite<sup>®</sup> M1000 at 405 nm. A standard curve was prepared using prescribed concentrations of p-nitrophenol as per Abcam instructions. The blank absorbance reading was subtracted from each data point and, via the standard curve, ALP activity was determined.

## 2.7. Statistical analysis

Statistical analysis was performed using the programming language, R, using a two-way ANOVA at a significance of  $\alpha = 0.05$  and Tukey's HSD test was used to evaluate contrasts. All in vitro data was accepted to be normally distributed as per the Shapiro-Wilk test ( $p > 0.05$ ).

## 3. Results and discussion

In order to combine the advantageous properties of PLL, such as cell adhesion and proliferation, with the unique adhesive properties of catechol, we modified PLL with the catechol-containing molecule DHBA (Fig. 1). The chemical structure of DHBA consists of a catechol group attached to an aldehyde, which makes it well suited for attachment to the amine group via Schiff base reaction, building on our previous work with chitosan [11]. In a Schiff base reaction, the amine group acts as a nucleophile and attacks the aldehyde group in DHBA. The nitrogen in the amine replaces the oxygen in the carbonyl group, and as a result the PLL monomer is modified with a catechol group. The chemical structure of the modified PLL monomer can be seen in Fig. 1C. In the present work, PLL-DHBA films were fabricated using cathodic EPD, which is governed by the local pH increase at the electrode surface (described by Eq. (1)).

The presence of a Schiff base was confirmed using UV-vis and Fourier Transform Infrared (FTIR) spectroscopy, as features from both the PLL and DHBA spectra can be found in both the PLL-DHBA UV-vis and FTIR spectra (Fig. 2 and Supporting Information Figure S1). In the UV-vis spectra, the absorptions between 250 and 350 nm are characteristic of the catechol group in DHBA [17]. These characteristic catechol absorptions are not found in the pure PLL spectra but can be found in the spectra of PLL-DHBA, which is indicative that PLL monomers were successfully modified with DHBA. The PLL-DHBA spectrum

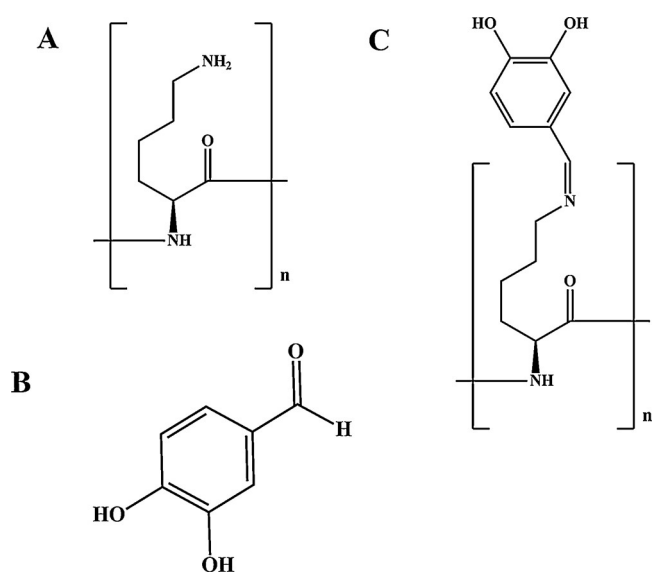


Fig. 1. Chemical structure of (A) PLL, (B) DHBA and (C) PLL-DHBA.

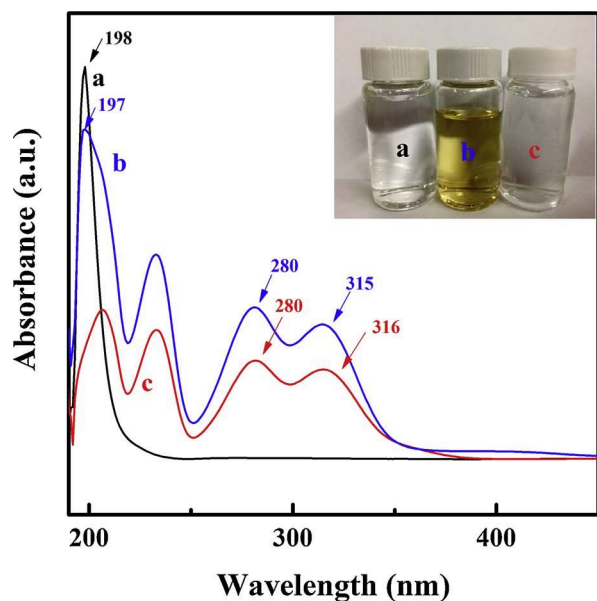


Fig. 2. UV-vis spectra of (a) PLL, (b) DHBA and (c) PLL-DHBA. Insert: (a) pure PLL, (b) PLL-DHBA, and (c) pure DHBA in solution.

also contains a large absorption with a maxima around 197 nm, which is also found in the pure PLL spectra [18] and indicates that both PLL and DHBA are present. The FTIR spectra also confirmed modification of the PLL monomer with catechol, as it revealed characteristic absorbances at approximately 2854 and 2921  $\text{cm}^{-1}$  from DHBA in accordance with the manufacturer's specifications. Characteristic absorbances from the pure poly-L-lysine spectra were also observed, such as NH and C=O at 1530 and 1650  $\text{cm}^{-1}$ , respectively [4]. The presence of Schiff base formation is also indicated by a solution colour change, from clear to yellow (Fig. 2 inset).

Past experiments have found that catechol-containing molecules allow for superior adsorption to the surface of metal, metal oxide and hydroxide particles [19]. Superior coating adhesion was also observed in the present study, with all coatings achieving 5B classification according to the ASTM D3359-09 Tape Test, which is the highest level of adhesion (Supporting Information, Figure S2). The adsorption of catechol is not only advantageous for increasing coating adhesion, but also for the fabrication of composite coatings using EPD, because the adsorbed organic molecule imparts an electric charge to the particles. This allows for improved dispersion via electrostatic repulsion. It has been suggested that the mechanism of catechol adsorption on metal oxide or hydroxide particles involves interaction between the hydroxyl groups of the catechol moiety and metallic atoms on the inorganic particle surface [19]. It can be inferred that a similar adsorption mechanism is at play between PLL-DHBA and Ca or Ti atoms in the HA or  $\text{TiO}_2$  nanoparticle surface. Catechol adsorption has two possible configurations: bridging or chelating. A schematic diagram of these two adsorption configurations of PLL-DHBA and either Ca or Ti can be found in Figure S3 in the supporting information.

In the present study, the functionalization of PLL with DHBA allowed for catecholate bonding, which resulted in improved adsorption of PLL-DHBA on the HA or  $\text{TiO}_2$  particle surface. PLL-DHBA was used as a dispersing, charging, and film forming agent. Thick composite films, containing HA,  $\text{TiO}_2$ , or both HA and  $\text{TiO}_2$  were deposited. XRD was used to confirm co-deposition of HA and  $\text{TiO}_2$ , and X-ray diffraction patterns of PLL-DHBA-HA, PLL-DHBA- $\text{TiO}_2$ , and PLL-DHBA-HA- $\text{TiO}_2$  can be seen in Fig. 3. Sharp peaks were observed for both HA and  $\text{TiO}_2$ , which confirmed the fabrication of the coating containing both bio-ceramics. Many efforts have been made to develop organic-inorganic nano-composite coatings to improve the osseointegration of orthopaedic

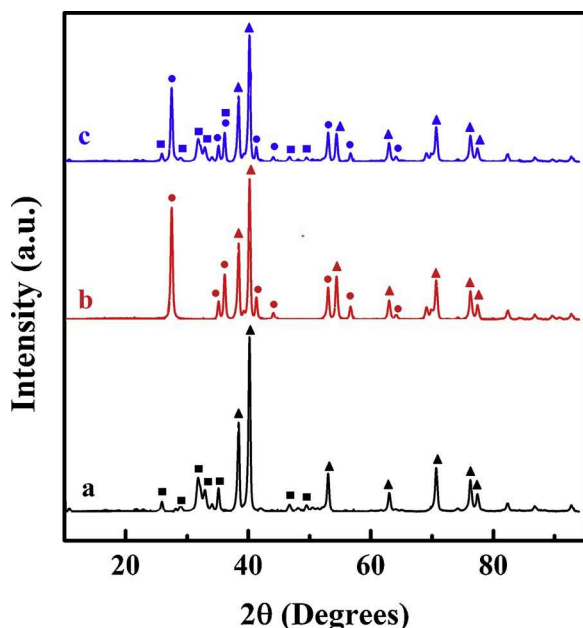


Fig. 3. X-ray diffraction patterns for (a) PLL-DHBA-HA, (b) PLL-DHBA- $\text{TiO}_2$  and (c) PLL-DHBA-HA- $\text{TiO}_2$ , (■ – corresponds to JCPDS file 00-024-0033 for HA, ● – corresponds to JCPDS file 01-089-0553  $\text{TiO}_2$ , and ▲ – corresponds to JCPDS file 00-044-1294 for Ti substrate).

implant materials via the incorporation of bioactive bioceramic materials, but it is also known that the surface roughness and contact angle also have a strong effect [20]. It has been found previously that lower contact angles, and thus greater hydrophilicity, and increased surface roughness of biomedical implant coatings improves osseointegration [20]. More recently it has been determined that surface topography has a strong influence on osteoblast adhesion and proliferation, and that a dual scale topography, one that includes both nano- and microscale features is optimal for promoting osteoblast adhesion [21–23]. A variety of treatments have been used previously to introduce nano-scale roughness to previously fabricated micro-scale features, including electrochemical etching, sand-blasting and acid-etching [21]. In the present study, we have obtained dual scale topography in one step (Fig. 4). As can be seen in the low-magnification SEM images, all coatings exhibited micro-scale “clusters” of HA,  $\text{TiO}_2$  or HA and  $\text{TiO}_2$  nanoparticles within the PLL-DHBA matrix (Fig. 4A and B for HA coatings, supporting information Figure S4 for all other coatings). At higher magnification, we can see in the SEM images that the nano-particles are well-dispersed within the PLL-DHBA matrix and thus provide features at both the nano- and micro-scale for cell interaction. AFM was used to further study the surface morphology of the PLL-DHBA-HA, PLL-DHBA- $\text{TiO}_2$  and PLL-DHBA-HA- $\text{TiO}_2$  coatings. Three-dimensional reconstructions of the surface can be found in Fig. 5. It can be seen from the surface reconstructions that all coatings exhibited topography on the micrometer scale. The average surface roughness results can be found in Table 1. PLL-DHBA-HA- $\text{TiO}_2$  exhibited the greatest average roughness, followed by PLL-DHBA- $\text{TiO}_2$  and PLL-DHBA-HA. It has been reported that the optimal average roughness for dental implant surfaces lies within 0.5  $\mu\text{m}$  and 1.0  $\mu\text{m}$  [20], the average roughness of all composite films fell within this range, with the exception of PLL-DHBA-HA- $\text{TiO}_2$ . These results combined with SEM characterization confirmed that we achieved the desired dual-scale topography for all three coatings. We hypothesize that this unique surface topography was achieved in one-step due to our choice of relatively high deposition voltage. Previous investigations by our group used a deposition voltage of 10 V for the fabrication of pure PLL-HA composite films, and smooth, uniform films were achieved [13]. This is in sharp contrast to the films that were fabricated in this study, which used a deposition voltage of 50 V and exhibited rough surface topography. In a previous study, it was discovered that the coating porosity of pure HA increased with increasing voltage when deposited using EPD [15]. When low voltages were used for deposition, it resulted in the preferred deposition of small particles, but a larger range of particle sizes were deposited at higher voltages [15]. Coatings with greater porosity were also achieved at

higher voltages. These changes in surface morphology and particle size, that were observed with an increase in voltage, can be attributed to the tendency of particles to partially agglomerate with the application of a stronger electric field, as well as the increased hydrogen evolution at the cathode surface [15].

In addition to exhibiting surface roughness and dual-scale topography, the surface wettability must also be increased in order to promote cell proliferation and adhesion [20]. Simultaneously increasing the surface roughness and wettability has proved challenging, as techniques such as acid-etching and grit-blasting have been found to greatly increase hydrophobicity in titanium dental implant materials [24]. It is hypothesized that this increase in contact angle was a result of air trapped below the wetting liquid, and a variety of additional surface modification techniques have been developed to decrease the contact angle while maintaining surface roughness, such as modification with polyelectrolytes, plasma or alkaline surface treatments [24]. Contact angle measurements determined that the presence of inorganic nanoparticles increased the wettability of PLL-DHBA (Supporting Information Figure S5 and Table 1). PLL-DHBA-HA exhibited the smallest contact angle, followed by PLL-DHBA-TiO<sub>2</sub> and PLL-HA-TiO<sub>2</sub>. The observed decrease in contact angle following the addition of ceramic nanoparticles could be attributed to the subsequent increase in porosity, compared to pure PLL-DHBA. This effect was observed comparing in the literature when characterizing alginate/bioglass® coatings, and it was realized that coatings with micron-sized pores and high porosity achieve increased surface wettability, since the water droplet can more easily penetrate the coating structure [25].

In a previous study that measured the relationship between

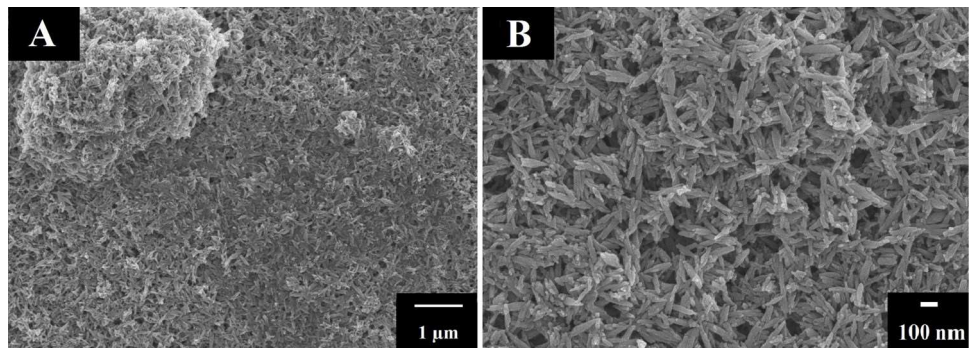


Fig. 4. SEM images of PLL-DHBA-HA coatings at (A) low and (B) high magnification, exhibiting dual-scale topography.

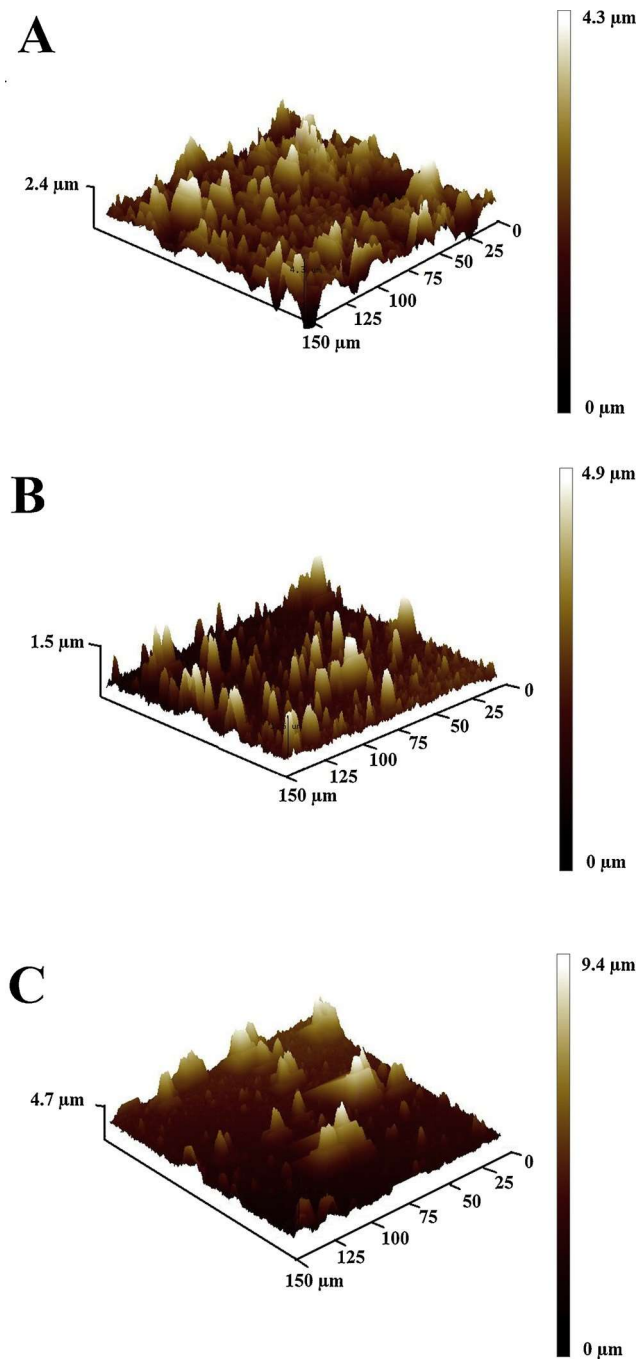


Fig. 5. AFM results for (A) PLL-DHBA-HA, (B) PLL-DHBA-TiO<sub>2</sub> and (C) PLL-DHBA-HA-TiO<sub>2</sub>. PLL-DHBA-HA-TiO<sub>2</sub> exhibited the greatest surface roughness, followed by PLL-DHBA-HA and then PLL-DHBA-TiO<sub>2</sub>.

Table 1  
Comparison of average contact angles and average roughness for PLL-DHBA coatings.

Coating	Average Contact Angle (°)	Average Roughness (μm)
PLL-DHBA	53.8 ± 5	0.046 ± 0.02
PLL-DHBA-HA	20.8 ± 10	0.900 ± 0.06
PLL-DHBA-TiO <sub>2</sub>	33.8 ± 4	0.942 ± 0.04
PLL-DHBA-HA-TiO <sub>2</sub>	47.8 ± 9	1.21 ± 0.10

wettability, protein absorption and cell adhesion, it was found that the optimal contact angle range lies between 30-60° [24]. The contact angles of all our bioceramic-containing coatings measured in this study had an average contact angle within this optimal range, with the exception of the PLL-DHBA-HA coatings, which had an average contact angle slightly below this threshold.

The cell metabolism results are shown in Fig. 6A which approximate fluorescence to cell metabolism. For all EPD films, the cell metabolism increased in magnitude from 1 to 3 days, however, this was only statistically significant for the PLL-DHBA-TiO<sub>2</sub> film ( $p < 0.05$ ). Additionally, at the 3-day time point, the PLL-DHBA-TiO<sub>2</sub> film showed significantly increased metabolism compared to both the PLL-DHBA-HA and PLL-DHBA-HA-TiO<sub>2</sub> films ( $p < 0.05$ ).

Alkaline phosphatase activity, Fig. 6B, was shown, similar to cell metabolism, to increase in magnitude from 1 to 3 days for both the PLL- DHBA-TiO<sub>2</sub> and PLL-DHBA-HA-TiO<sub>2</sub> films. Similar to cell metabolism, the PLL-DHBA-TiO<sub>2</sub> film showed a statistically significant increase from 1 to 3 days ( $p < 0.05$ ) and at 3 days had more ALP activity than both PLL-DHBA-HA and PLL-DHBA-HA-TiO<sub>2</sub> films ( $p < 0.05$ ). Overall, the effects observed in ALP activity correspond directly to cell metabolism results.

*In vitro* results demonstrated that the EPD films did not have noticeable cytotoxic effects when considering cell metabolism and alkaline phosphatase activity. The PLL-DHBA-TiO<sub>2</sub> film showed improved cell metabolism and alkaline phosphatase activity than both the PLL- DHBA-HA and PLL-DHBA-HA-TiO<sub>2</sub> films at 3 days and was the only film to show a statistically significant increase from 1 to 3 days. Previous studies have suggested that nanoscale HA particles may have cytotoxic effects which may be a contributing reason for the lack of statistically significant changes for the EPD films containing HA [26,27]. The HA nanorods used in the films had an average width of  $31 \pm 1.4$  nm, and an average length of  $169 \pm 15$  nm. Other authors have found that similar sized nanorods were relatively non-cytotoxic [28]. However, despite these concerns, the films containing HA were not cytotoxic as demonstrated by the maintained cell metabolism and ALP activity results. HA films and deposition have a history of being successfully used in biomaterials with success, so it is possible that the observation period was too short to elucidate the response of the HA films [29,30]. As a preliminary *in vitro* analysis, it could be concluded that the PLL-DHBA- TiO<sub>2</sub> film performed better than the other films. TiO<sub>2</sub> particles and films have both demonstrated improved response from bone cells in the past which is agreeable with the results of this study [31,32]. This is supported by the contact angle data which shows that the films are hydrophilic which is generally considered beneficial for early biomaterial- tissue interactions [31]. The sub-micron roughness of the surface, contributed from both meso- and nanoparticles, matches previous studies which support the use of dual-topographies in implant-based materials [33–35]. Going forward, additional studies using longer time points, alternative cell lines and perhaps *in vivo* work will be necessary to understand the cellular responses to these dual-topography EPD films.

#### 4. Conclusions

For the first time we demonstrate a novel one-step fabrication technique for the development of catechol-modified PLL nanocomposite films that exhibit dual nano- and micro-scale topography with high wettability. Our modification technique utilizes a Schiff base reaction to modify L-lysine monomers with a catechol group, using the catechol- containing DHBA molecule. This new method allows for the co-de- position of both HA and TiO<sub>2</sub>, combining the bioactivity of HA with the biocompatibility and stability of TiO<sub>2</sub>. Our new strategy for co-dispersion and deposition is based on biomimetic catecholate type bonding, which significantly increases adhesion compared to pure PLL which exhibits weak adsorption to inorganic particles. This technique also achieves dual-scale topography in one-step, with the use of cathodic electrophoretic deposition at a relatively high voltage (50 V). All composite coatings fabricated were found to be hydrophilic in addition.

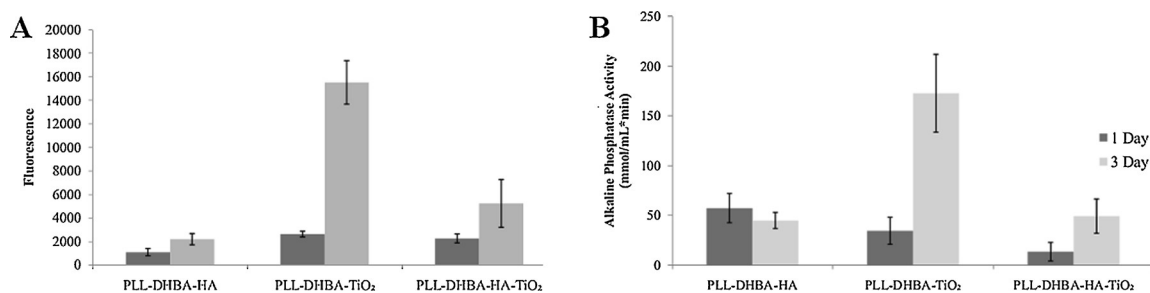


Fig. 6. (A) Cell metabolism results for EPD films at 1 and 3-day time points. Cell metabolism showed significant increases from 1 to 3 days for the PLL-DHBA-TiO<sub>2</sub> film only ( $p < 0.05$ ). Additionally, the PLL-DHBA-TiO<sub>2</sub> film demonstrated significantly greater cell metabolism at 3 days compared to the other EPD films. Errors bars represent standard deviation. (B) ALP activity results for EPD films at 1 and 3-day time points. ALP activity showed significant increases from 1 to 3 days for the PLL-DHBA-TiO<sub>2</sub> film only ( $p < 0.05$ ). The PLL-DHBA-TiO<sub>2</sub> film demonstrated significantly greater ALP activity at 3 days compared to the other EPD films ( $p < 0.05$ ).

to exhibiting high surface roughness, which is advantageous for osteoblast attachment and proliferation. *in vitro* testing revealed that all coatings studied were not cytotoxic and showed an increase in cell metabolism as well as alkaline phosphatase activity in the studied time period. This work paves the way for the next generation of biomedical implants with improved osseointegration and increased lifespan.

#### Acknowledgements

The authors gratefully acknowledge the Natural Sciences and Engineering Research Council of Canada for the financial support and Bionterfaces Institute of McMaster University for the cell studies.

#### Appendix A. Supplementary data

Supplementary material related to this article can be found, in the online version, at doi:<https://doi.org/10.1016/j.colsurfb.2018.12.049>.

## References

- [1] N. Sahiner, Single step poly(L-Lysine) microgel synthesis, characterization and biocompatibility tests, *Polymer (United Kingdom)* 121 (2017) 46–54, <https://doi.org/10.1016/j.polymer.2017.06.014>.
- [2] Z. Tan, T. Bo, F. Guo, J. Cui, S. Jia, Effects of  $\epsilon$ -Poly-L-lysine on the cell wall of *Saccharomyces cerevisiae* and its involved antimicrobial mechanism, *Int. J. Biol. Macromol.* 118 (Part B) (2018) 2230–2236, <https://doi.org/10.1016/j.ijbiomac.2018.07.094>.
- [3] G. Sun, Q. Yang, A. Zhang, J. Guo, X. Liu, Y. Wang, Q. Ma, Synergistic effect of the combined bio-fungicides  $\epsilon$ -poly-L-lysine and chitoooligosaccharide in controlling grey mould (*Botrytis cinerea*) in tomatoes, *Int. J. Food Microbiol.* 276 (2018) 46–53, <https://doi.org/10.1016/j.ijfoodmicro.2018.04.006>.
- [4] M. Kouhi, M. Fathi, M.P. Prabhakaran, M. Shamanian, S. Ramakrishna, Poly L lysine-modified PHBV based nanofibrous scaffolds for bone cell mineralization and osteogenic differentiation, *Appl. Surf. Sci.* 457 (2018) 616–625, <https://doi.org/10.1016/j.apsusc.2018.06.239>.
- [5] M. Mekhail, K. Jahan, M. Tabrizian, Genipin-crosslinked chitosan/poly-L-lysine gels promote fibroblast adhesion and proliferation, *Carbohydr. Polym.* 108 (2014) 91–98, <https://doi.org/10.1016/j.carbpol.2014.03.021>.
- [6] X. Wang, H. Zhang, H. Jing, L. Cui, Highly efficient labeling of human lung Cancer cells using cationic Poly-L-lysine-Assisted magnetic Iron oxide nanoparticles, *Nano-Micro Lett.* 7 (2015) 374–384, <https://doi.org/10.1007/s40820-015-0053-5>.
- [7] H. Jin, Y. Yu, W.B. Chrisler, Y. Xiong, D. Hu, C. Lei, Delivery of microRNA-10b with polylysine nanoparticles for inhibition of breast cancer cell wound healing, *Breast Cancer Basic Clin. Res.* 5 (2011) 9–19, <https://doi.org/10.4137/BCBCR.S8513>.
- [8] L. Li, H. Zeng, Marine mussel adhesion and bio-inspired wet adhesives, *Biotribology* 5 (2016) 44–51, <https://doi.org/10.1016/j.biotri.2015.09.004>.
- [9] J. Hyun, S. Hong, H. Lee, *Acta Biomaterialia* Bio-inspired adhesive catechol-conjugated chitosan for biomedical applications : a mini review, *Acta Biomater.* 27 (2015) 101–115, <https://doi.org/10.1016/j.actbio.2015.08.043>.
- [10] T.E. Winkler, H. Ben-Yoav, S.E. Chocron, E. Kim, D.L. Kelly, G.F. Payne, R. Ghodssi, Electrochemical study of the catechol-modified chitosan system for clozapine treatment monitoring, *Langmuir* 30 (2014) 14686–14693, <https://doi.org/10.1021/la503529k>.
- [11] A. Clifford, X. Pang, I. Zhitomirsky, Biomimetically modified chitosan for electrophoretic deposition of composites, *Colloids Surfaces A Physicochem. Int. J. Pavement Eng. Asph. Technol.* 544 (2018) 28–34, <https://doi.org/10.1016/j.colsurfa.2018.02.028>.
- [12] A.R. Boccaccini, S. Keim, R. Ma, Y. Li, I. Zhitomirsky, Electrophoretic deposition of biomaterials, *J. R. Soc. Interface* 7 (2010) S581–S613, <https://doi.org/10.1098/rsif.2010.0156.focus>.
- [13] Y. Wang, X. Pang, I. Zhitomirsky, Electrophoretic deposition of chiral polymers and composites, *Colloids Surf. B Biointerfaces* 87 (2011) 505–509, <https://doi.org/10.1016/j.colsurfb.2011.05.043>.
- [14] A. Szcześ, L. Hofysz, E. Chibowski, Synthesis of hydroxyapatite for biomedical applications, *Adv. Colloid Interface Sci.* 249 (2017) 321–330, <https://doi.org/10.1016/j.cis.2017.04.007>.
- [15] I. Zhitomirsky, L. Gal-Or, Electrophoretic deposition of hydroxyapatite, *J. Mater. Sci. Mater. Med.* 8 (1997) 213–219, <https://doi.org/10.1023/A:1018587623231>.
- [16] B.E.J. Lee, H. Exir, A. Weck, K. Grandfield, Characterization and evaluation of femtosecond laser-induced sub-micron periodic structures generated on titanium to improve osseointegration of implants, *Appl. Surf. Sci.* 441 (2018) 1034–1042, <https://doi.org/10.1016/j.apsusc.2018.02.119>.
- [17] M. Andjelković, J. Van Camp, B. De Meulenaer, G. Depaemelaere, C. Socaciu, M. Verloo, R. Verhe, Iron-chelation properties of phenolic acids bearing catechol and galloyl groups, *Food Chem.* 98 (2006) 23–31, <https://doi.org/10.1016/j.foodchem.2005.05.044>.
- [18] C. Shan, H. Yang, D. Han, Q. Zhang, A. Ivaska, L. Niu, Water-soluble graphene covalently functionalized by biocompatible poly-L-lysine, *Langmuir* 25 (2009) 12030–12033, <https://doi.org/10.1021/la903265p>.
- [19] M.S. Ata, Y. Liu, I. Zhitomirsky, A review of new methods of surface chemical modification, dispersion and electrophoretic deposition of metal oxide particles, *RSC Adv.* 4 (2014) 22716–22732, <https://doi.org/10.1039/c4ra02218a>.
- [20] C.N. Elias, Y. Oshida, J.H.C. Lima, C.A. Muller, Relationship between surface properties (roughness, wettability and morphology) of titanium and dental implant removal torque, *J. Mech. Behav. Biomed. Mater.* 1 (2008) 234–242, <https://doi.org/10.1016/j.jmbbm.2007.12.002>.
- [21] K. Gulati, M. Prideaux, M. Kogawa, L. Lima-Marques, G.J. Atkins, D.M. Findlay, D. Losic, Anodized 3D-printed titanium implants with dual micro- and nano-scale topography promote interaction with human osteoblasts and osteocyte-like cells, *J. Tissue Eng. Regen. Med.* 11 (2017) 3313–3325, <https://doi.org/10.1002/term.2239>.
- [22] I.J. Macha, B. Ben-Nissan, J. Santos, S. Cazalbou, A. Stamboulis, D. Grossin, G. Giordano, Biocompatibility of a new biodegradable polymer-hydroxyapatite composite for biomedical applications, *J. Drug Deliv. Sci. Technol.* 38 (2017) 72–77, <https://doi.org/10.1016/j.jddst.2017.01.008>.
- [23] B.E.J. Lee, S. Ho, G. Mestres, M. Karlsson Ott, P. Koshy, K. Grandfield, Dual-topography electrical discharge machining of titanium to improve biocompatibility, *Surf. Coatings Technol.* 296 (2016) 149–156, <https://doi.org/10.1016/j.surfcoat.2016.04.024>.
- [24] F. Rupp, L. Liang, J. Geis-Gerstorf, L. Scheideler, F. Hüttig, Surface characteristics of dental implants: a review, *Dent. Mater.* 34 (2018) 40–57, <https://doi.org/10.1016/j.dental.2017.09.007>.
- [25] Q. Chen, L. Cordero-Arias, J.A. Roether, S. Cabanas-Polo, S. Virtanen, A.R. Boccaccini, Alginate/Bioglass® composite coatings on stainless steel deposited by direct current and alternating current electrophoretic deposition, *Surf. Coat. Technol.* 233 (2013) 49–56, <https://doi.org/10.1016/j.surfcoat.2013.01.042>.
- [26] X. Zhao, S. Ng, B.C. Heng, J. Guo, L. Ma, T.T.Y. Tan, K.W. Ng, S.C.J. Loo, Cytotoxicity of hydroxyapatite nanoparticles is shape and cell dependent, *Arch. Toxicol.* 87 (2013) 1037–1052, <https://doi.org/10.1007/s00204-012-0827-1>.
- [27] M. Motskin, D.M. Wright, K. Muller, N. Kyle, T.G. Gard, A.E. Porter, J.N. Skepper, Hydroxyapatite nano and microparticles: correlation of particle properties with cytotoxicity and biostability, *Biomaterials* 30 (2009) 3307–3317, <https://doi.org/10.1016/j.biomaterials.2009.02.044>.
- [28] J. Scheel, S. Weimans, A. Thiemann, E. Heisler, M. Hermann, Exposure of the murine RAW 264.7 macrophage cell line to hydroxyapatite dispersions of various composition and morphology: assessment of cytotoxicity, activation and stress response, *Toxicol. In Vitro* 23 (2009) 531–538, <https://doi.org/10.1016/j.tiv.2009.01.007>.
- [29] R.M.G. Rajapakse, W.P.S.L. Wijesinghe, M.M.M.G.P.G. Mantilaka, K.G. Chathuranga Senarathna, H.M.T.U. Herath, T.N. Premachandra, C.S.K. Ranasinghe, R.P.V.J. Rajapakse, M. Edirisinghe, S. Mahalingam, I.M.C.C.D. Bandara, S. Singh, Preparation of bone-implants by coating hydroxyapatite nanoparticles on self-formed titanium dioxide thin-layers on titanium metal surfaces, *Mater. Sci. Eng. C* 63 (2016) 172–184, <https://doi.org/10.1016/j.msec.2016.02.053>.
- [30] H. Zhou, J. Lee, Nanoscale hydroxyapatite particles for bone tissue engineering, *Acta Biomater.* 7 (2011) 2769–2781, <https://doi.org/10.1016/j.actbio.2011.03.019>.
- [31] T. Shinonaga, M. Tsukamoto, A. Nagai, K. Yamashita, T. Hanawa, N. Matsushita, G. Xie, N. Abe, Cell spreading on titanium dioxide film formed and modified with aerosol beam and femtosecond laser, *Appl. Surf. Sci.* 288 (2014) 649–653, <https://doi.org/10.1016/j.apsusc.2013.10.090>.
- [32] H. Te Chen, H.Y. Shu, C.J. Chung, J.L. He, Assessment of bone morphogenic protein and hydroxyapatite-titanium dioxide composites for bone implant materials, *Surf. Coatings Technol.* 276 (2015) 168–174, <https://doi.org/10.1016/j.surfcoat.2015.06.056>.
- [33] K. Grandfield, Bone, implants, and their interfaces, *Phys. Today* 68 (2015) 40–45, <https://doi.org/10.1063/PT.3.2748>.
- [34] C. Eriksson, H. Nygren, K. Ohlson, Implantation of hydrophilic and hydrophobic titanium discs in rat tibia: Cellular reactions on the surfaces during the first 3 weeks in bone, *Biomaterials* 25 (2004) 4759–4766, <https://doi.org/10.1016/j.biomaterials.2003.12.006>.
- [35] F.A. Shah, B. Nilsson, R. Bränemark, P. Thomsen, A. Palmquist, The bone-implant interface - nanoscale analysis of clinically retrieved dental implants, *Nanomedicine Nanotechnology, Biol. Med.* 10 (2014) 1729–1737, <https://doi.org/10.1016/j.nano.2014.05.015>.